Supplementary Data

Excitation dependent white and red-NIR emission of Mn^{II}-based complex

Wiem Jabeur[a], Rawia Msalmi[a], Marcus Korb[b], Fredj Hassen[c], Ahlem Guesmi[d], Ammar Houas[e], Naoufel Ben Hamadi[d,f] and Houcine Naïli[a]*

[a] *Laboratory Physico Chemistry of the Solid State, Department of Chemistry, Faculty of Sciences of Sfax, Sfax University, Tunisia.*

[b] *The University of Western Australia, School of Molecular Sciences, 35 Stirling Highway, Crawley, Perth, Western Australia 6009, Australia.*

[c] *Laboratoire de Micro-Optoélectronique et Nanostructures (LMON), Faculté des Sciences de Monastir, Université de Monastir, Avenue de l'environnement, Monastir, 5019, Tunisia.*

[d] *Chemistry Department, College of Science, IMSIU (Imam Mohammad Ibn Saud Islamic University), P.O. Box 5701, Riyadh 11432, Saudi Arabia.*

[e] *Research Laboratory of Catalysis and Materials for Environment and Processes, University of Gabes, City Riadh Zerig, Gabes, 6029, Tunisia.*

[f] *University of Monastir, Faculty of Science of Monastir, Laboratory of Heterocyclic Chemistry, Natural Products and Reactivity (LR11ES39), Team: Medicinal Chemistry and Natural Products, Avenue of Environment, 5019 Monastir, Tunisia.*

Table S1. Crystal data and structure refinement of $(AmpH)_2[MnCl_4(Apm)_2]$

Empirical formula	$C_{20}H_{30}Cl_4MnN_{12}$
Formula weight ($g.mol^{-1}$)	635.30
Wavelength	0.71073
Temperature (K)	121(4)
Crystal system	Triclinic
Space group	P-1
a (Å)	7.6700(8)
b (Å)	9.0452(10)
c (Å)	11.0423(10)
α (°)	108.104(9)
β (°)	96.967(9)
γ (°)	110.004(10)
V (Å3)	661.63(13)
Z	1
Calculated density (mg/m3)	1.594
Absorption coefficient (mm-1)	0.939
F(000)	327
Crystal size (mm3)	0.1 x 0.1 x 0.1
θ range for data collection (°)	2.923 to 24.998
h,k,l range	$-7 \leq h \leq 9$ $-10 \leq k \leq 10$ $-13 \leq l \leq 12$
Reflections number	2499
Absorption correction	Semi-empirical from equivalents
Transmission factors	T_{min}= 0.85249, T_{max}=1.00000
Number of parameters	192
Goodness of fit (F2)	1.066
R1	0.0453
wR2	0.1049
Largest diff. peak and hole (e.Å-3)	2.447 and -0.365

Table S2: Experimental and theoretical structural parameters for $(AmpH)_2[MnCl_4(Apm)_2]$

$[MnCl_4(C_5H_7N_3)_2]^{2-}$ complex					
Distance	Theoretical	Experimental	Angle	Theoretical	Experimental
Mn-Cl1	2.370	2.527(7)	Cl1-Mn-Cl2	89.009	91.20(2)
Mn-Cl2	2.424	2.574(7)	Cl1-Mn-Cl2(i)	90.991	88.80(2)
Mn-Cl1(i)	2.370	2.527(7)	Cl1(i)-Mn-Cl2	90.991	88.80(2)
Mn-Cl2(i)	2.424	2.574(7)	Cl1(i)-Mn-Cl2(i)	89.009	91.20(2)
Mn-N1	2.387	2.385(2)	N1-Mn-Cl2	88.285	88.29(5)
Mn-N1(i)	2.387	2.385(2)	N1-Mn-Cl1	88.935	88.60(5)
N1-C1	1.349	1.343(3)	N1-Mn-Cl1(i)	91.066	91.39(5)
C1-C2	1.407	1.381(4)	N1-Mn-Cl2(i)	91.715	91.71(5)
C2-C3	1.403	1.392(4)	N1(i)-Mn-Cl1	91.065	91.40(5)
C3-C4	1.512	1.497(3)	N1(i)-Mn-Cl2	91.715	91.71(5)
C3-N2	1.358	1.336(3)	N1(i)-Mn-Cl2(i)	88.285	88.29(5)
N2-C5	1.381	1.353(3)	N1(i)-Mn-Cl1(i)	88.934	88.61(5)
C5-N3	1.342	1.336(3)	Mn-N1-C1	114.312	113.26(15)
C5-N1	1.381	1.363(3)	Mn-N1-C5	127.952	131.15(17)
			C1-N1-C5	117.346	115.5(2)
			N1-C1-C2	122.707	123.9(2)
			C1-C2-C3	117.381	116.5(2)
			C2-C3-C4	122.216	121.3(2)
			C2-C3-N2	120.848	121.5(2)
			C4-C3-N2	116.937	117.2(2)
			C3-N2-C5	118.839	118.2(2)
			N3-C5-N2	118.007	116.8(2)
			N3-C5-N1	119.249	118.7(2)
			N2-C5-N1	122743	124.4(2)
$[C_5H_8N_3]^+$ cation					
N4-C6	1.402	1.345(4)	C10-N4-C6	120.754	121.3(2)
C6-C7	1.388	1.353(4)	N4-C6-C7	118.598	119.7(2)
C7-C8	1.419	1.416(4)	C6-C7-C8	119.218	117.7(3)
C8-C9	1.503	1.490(4)	C7-C8-C9	123.310	121.0(3)
C8-N5	1.379	1.325(3)	C9-C8-N5	116.230	117.1(2)
N5-C10	1.343	1.351(3)	C7-C8-N5	120.460	121.9(2)

C10-N6	1.348	1.317(4)	C8-N5-C10	120.527	118.8(2)
C10-N4	1.398	1.361(3)	N5-C10-N6	120.329	119.8(2)
			N5-C10-N4	120.441	120.5(2)
			N6-C10-N4	119.230	119.7(3)

Table S3. Hydrogen-bond geometry (Å, °).

D—H···A	d(D—H)(Å)	d(H···A)(Å)	d(D···A)(Å)	∠D—H···A(°)
N3–H1N···N5	0.87(3)	2.27(3)	3.138(4)	176(3)
N3–H2N···Cl2i	0.78(3)	2.44(3)	3.196(3)	163(3)
N6–H3N···N2	0.85(3)	2.09(3)	2.934(4)	178(4)
N6–H4N···Cl1ii	0.76(3)	2.45(3)	3.192(3)	165(3)
N4–H5N···Cl1ii	0.81(4)	2.76(4)	3.485(3)	150(3)
C6–H7··· Cl1iii	0.93	2.70	3.589(3)	160

Symmetry codes: (i) 1-x,2-y,-z ; (ii) x,y,1+z ; (iii) 2-x,2-y,1-z.

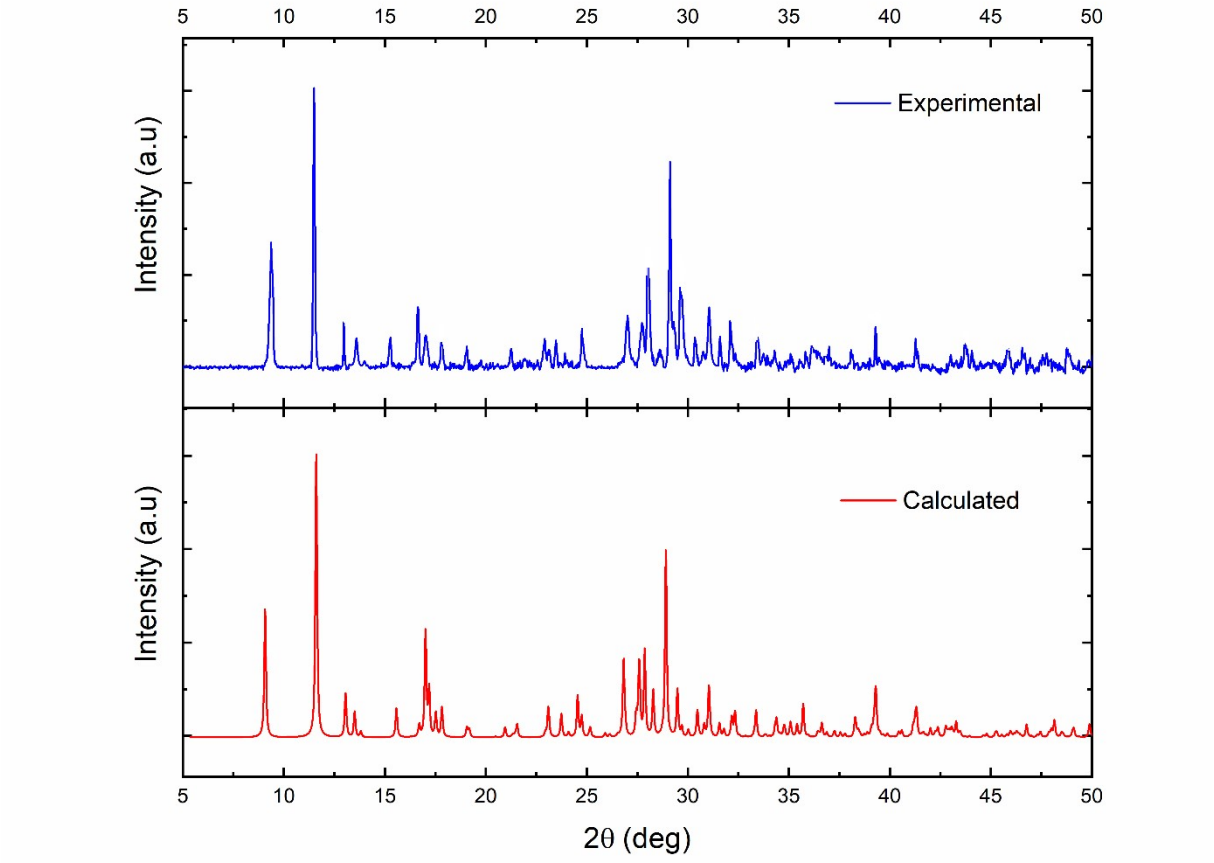

Fig. S1: Room temperature calculated and experimental X-ray diffraction patterns of $(AmpH)_2[MnCl_4(Apm)_2]$

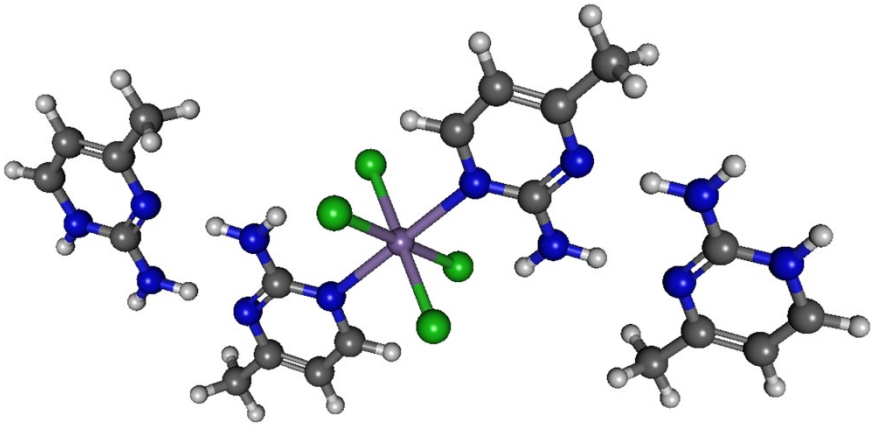

Fig. S2 The theoretical optimized geometry of the $(AmpH)_2[MnCl_4(Apm)_2]$.

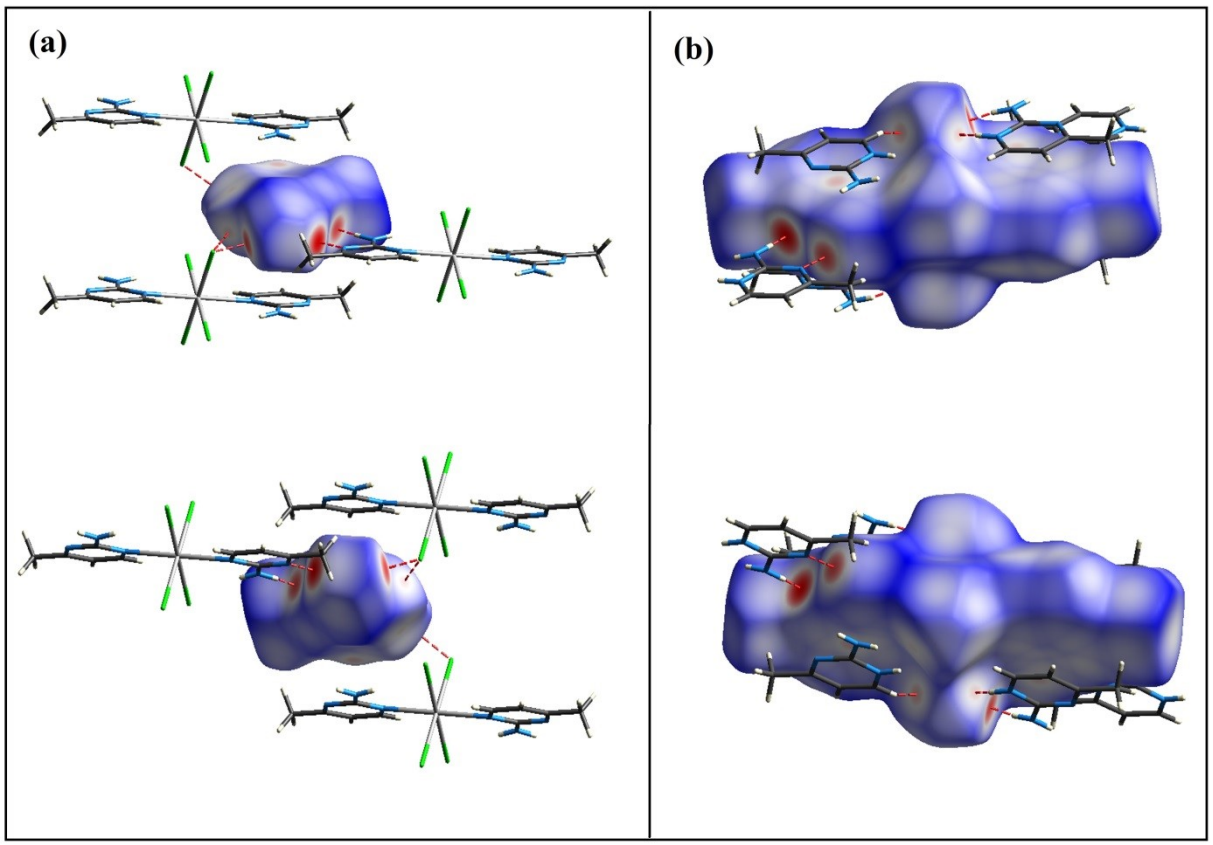

Fig. S3 Views of the Hirshfeld surface (back and front) for $[C_5H_8N_3]^+$ cation (a) and $[MnCl_4(C_5H_7N_3)_2]^{2-}$ anion (b)

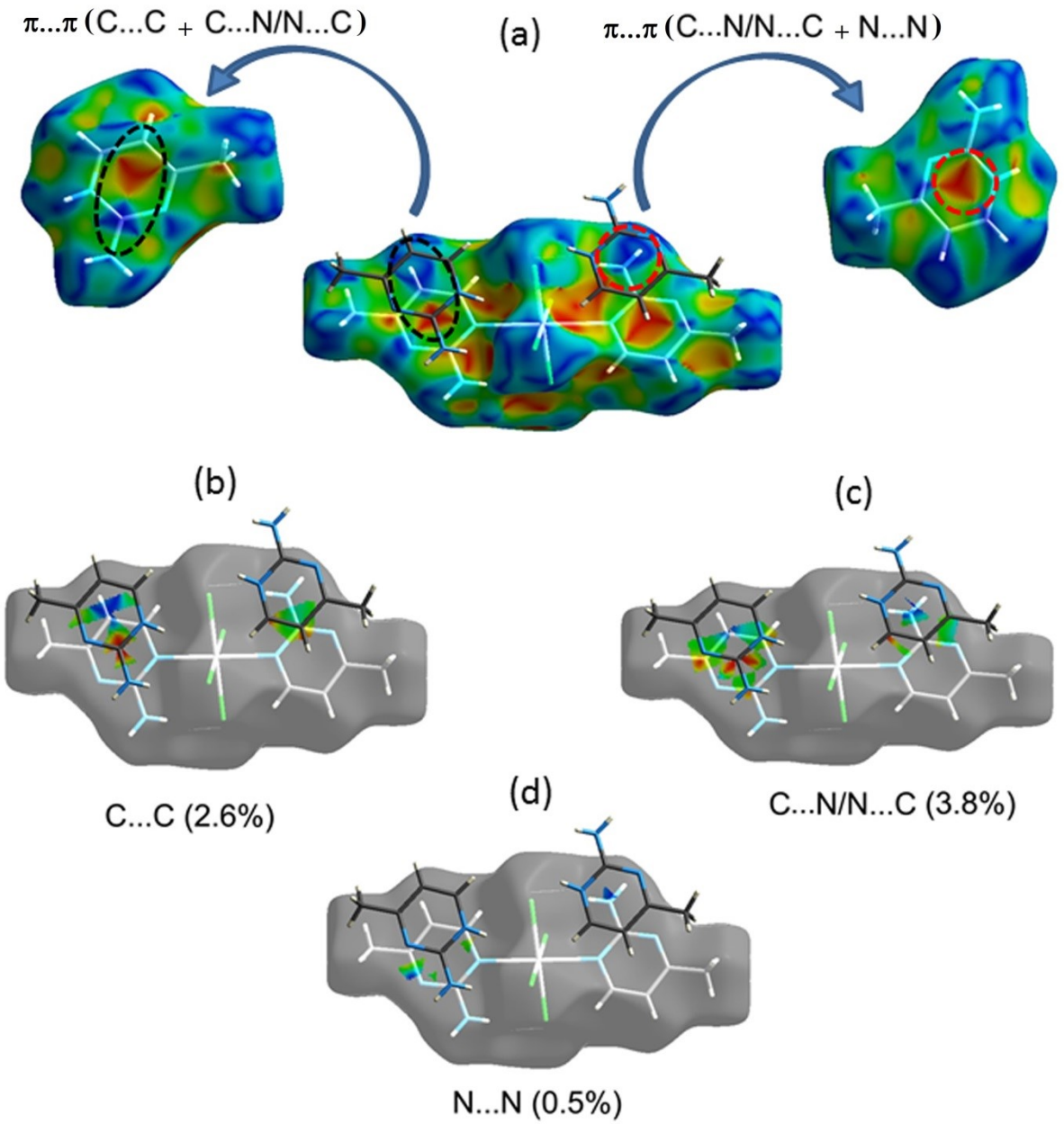

Fig. S4 Hirshfeld surfaces of the organic cations and the organometallic cluster mapped with shape index showing the detailed π-π type interactions. The red dashed circles and black dashed ellipses present the complementary regions characteristic of π-π interactions.

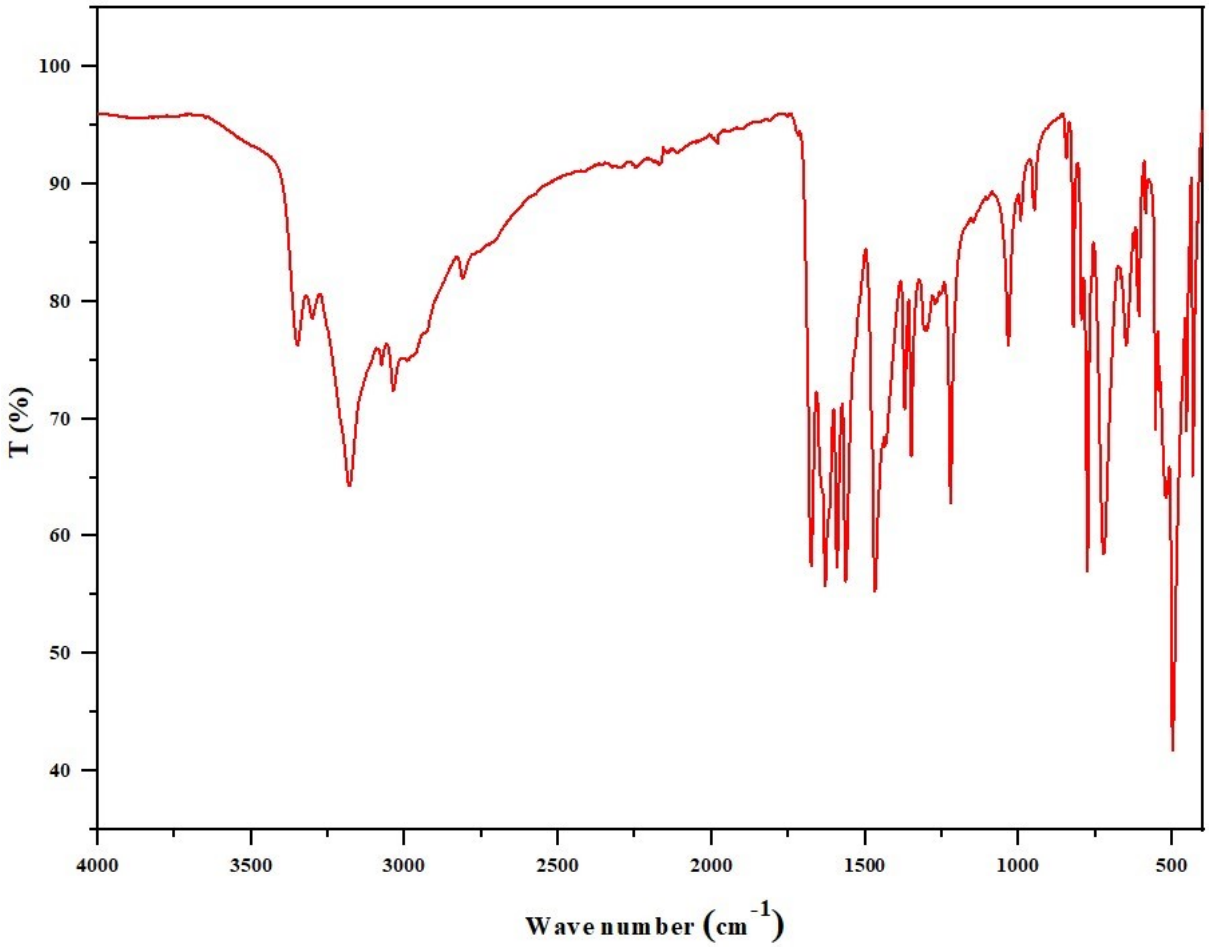

Fig. S5 The infrared absorption spectra of $(AmpH)_2[MnCl_4(Amp)_2]$, dispersed in a KBr pellet.

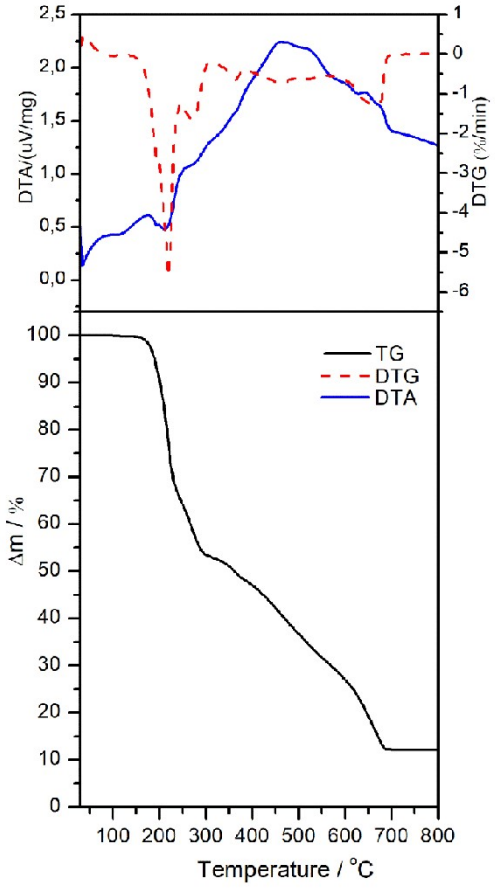

Fig. S6 Thermal analysis curves for the decomposition of $(AmpH)_2[MnCl_4(Amp)_2]$ (6 °C/min from 20 to 800 °C).

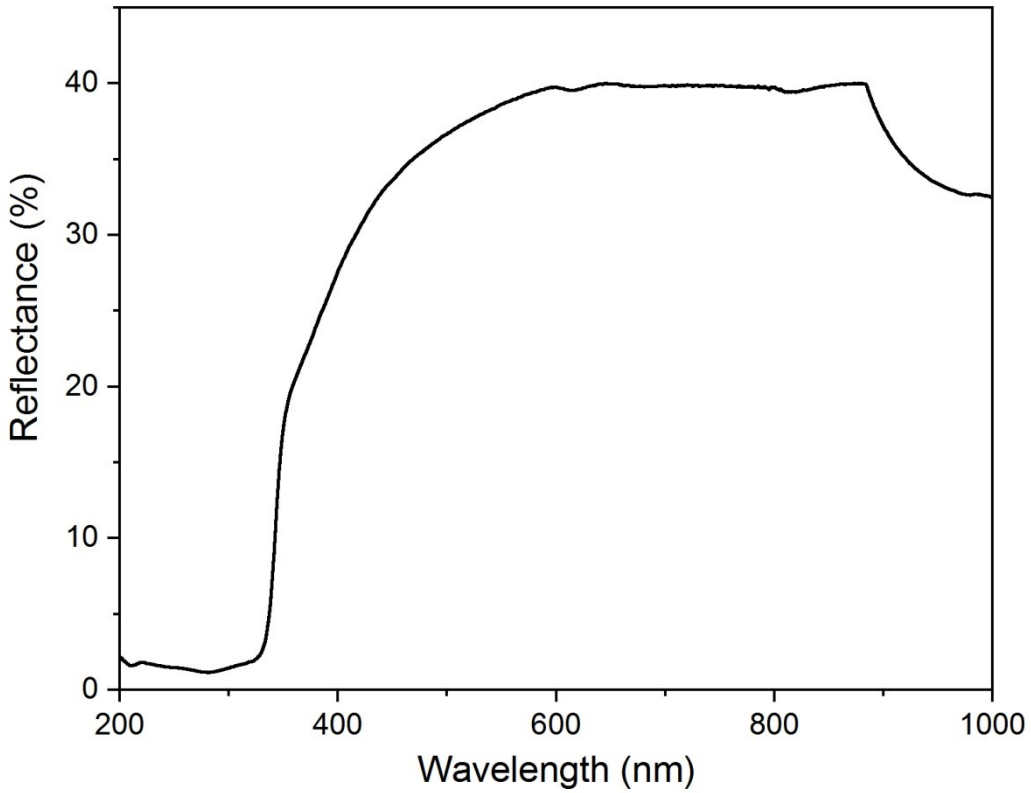

Fig. S7 UV-Vis-NIR Reflectance spectrum of $(AmpH)_2[MnCl_4(Apm)_2]$

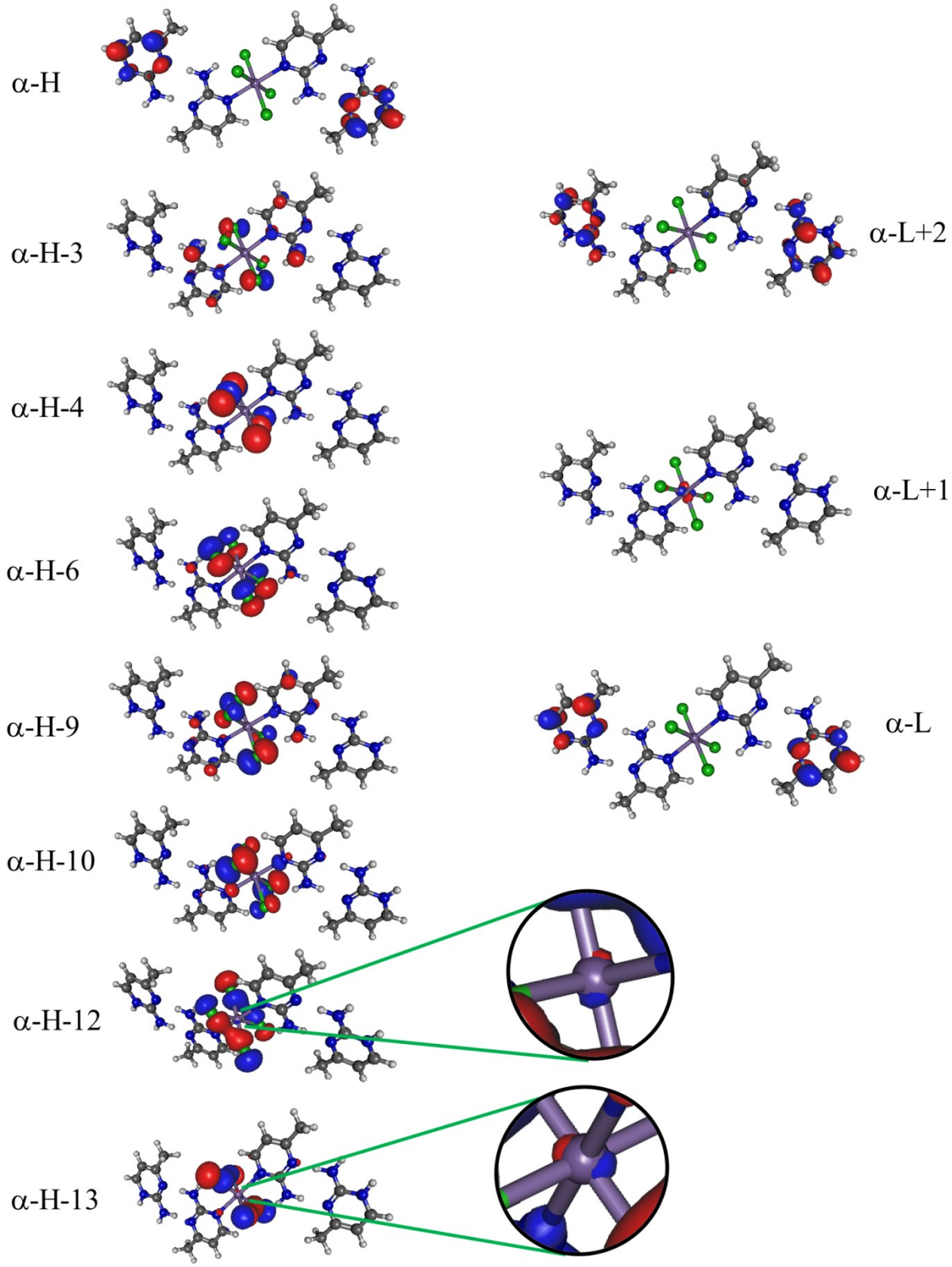

Fig. S8. The visualization of the alpha molecular orbitals contributed in the electronic transitions.

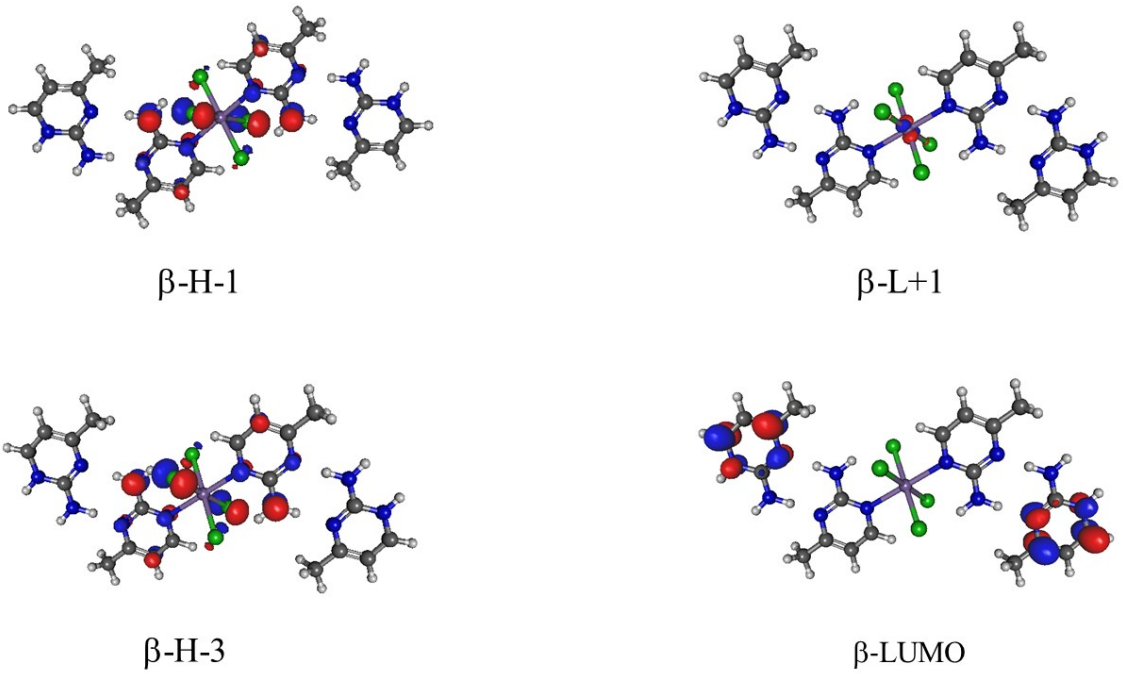

Fig. S9 The visualization of the beta molecular orbitals contributed in the electronic transitions.